

1
2
3
4
5
6
7
8
9
10
11
12
13
14
15
16
17
18
19
20
21
22
23
24
25
26
27
28
29
30
31
32
33
34
35
36
37
38
39
40
41
42
43
44

TITLE:

Live Imaging of Chemokine Receptors in Zebrafish Neutrophils during Wound Responses

AUTHORS AND AFFILIATIONS:

Antonios Georgantzoglou¹, Caroline Coombs¹, Hugo Poplimont^{1*}, Hazel A. Walker^{1*}, Milka Sarris¹

¹University of Cambridge, Department of Physiology, Development and Neuroscience, Downing Site, Cambridge, UK

*These authors contributed equally

Corresponding Author:

Milka Sarris (ms543@cam.ac.uk)

KEYWORDS:

zebrafish, chemokine, neutrophil, wound, imaging, microscopy

SUMMARY:

Here we describe protocols to perform live imaging and quantitative analysis of chemoattractant receptor dynamics in zebrafish neutrophils

ABSTRACT:

Leukocyte guidance by chemical gradients is essential for immune responses. Neutrophils are the first cells to be recruited to sites of tissue damage where they execute crucial antimicrobial functions. Their trafficking to these loci is orchestrated by a number of inflammatory chemoattractant, including chemokines. At the molecular level, chemoattractant signaling is regulated by the intracellular trafficking of the corresponding receptors. However, it remains unclear how subcellular changes in chemokine receptors affect leukocyte migration dynamics at the cell and tissue level. Here we describe a methodology for live imaging and quantitative analysis of chemokine receptor dynamics in neutrophils during inflammatory responses to tissue damage. These tools have revealed that differential chemokine receptor trafficking in zebrafish neutrophils coordinates neutrophil clustering and dispersal at sites of tissue damage. This has implications for our understanding of how inflammatory responses are self-resolved. The described tools could be used to understand neutrophil migration patterns in a variety of physiological and pathological settings and the methodology could be expanded to other signaling receptors.

INTRODUCTION:

Leukocyte migration is of paramount importance for immune responses. Immune cells are prototypical migratory cells, which are remarkably capable of traversing tissues and blood vessels and sensing a range of chemical guidance cues to migrate directionally towards microbes or other host cells of importance. Correct guidance relies on the recognition of chemoattractants, among which chemokines represent the most prominent category¹. Chemokines are recognized by

45 highly specific seven-transmembrane G protein coupled receptors. Upon chemokine binding,
46 chemokine receptors change conformation leading to the activation of associated trimeric G
47 proteins and their dissociation into functional signaling subunits that promote cytoskeletal
48 changes and directed migration¹. Secondly, chemokine receptors are phosphorylated, and this
49 modification leads to desensitization to attractant, which can be followed by rapid re-
50 sensitization/recycling or intracellular degradation and down-regulation from the cell surface².
51 These receptor dynamics influence the duration and dose of signaling received by the cells but
52 how they affect leukocyte migration behavior has been difficult to elucidate in vivo.

53
54 Tracking receptor dynamics in live leukocytes in traditional mammalian systems faces several
55 challenges. For live studies, receptor fusions with fluorescent proteins must be expressed in the
56 cells. This is challenging in primary leukocytes, particularly in neutrophils, and studies so far have
57 used surrogate neutrophil cell lines to express chemokine receptors^{3,4}. Generation of transgenic
58 mouse models, in which leukocytes express a fluorescent receptor or mutant receptors with
59 informative trafficking defects^{5,6}, entails considerable investment of time and resources. Even in
60 these instances, the imaging resolution and contrast for imaging receptor dynamics in the live
61 animal can be limited and studies have used immunohistochemistry on fixed tissue sections⁵.
62 Given these technical challenges, our understanding of how chemoattractant receptors dynamics
63 affect cell behavior in a live tissue setting is currently limited.

64
65 Here we provide a methodology to monitor receptor trafficking in zebrafish neutrophils.
66 Zebrafish are genetically tractable, like mice, but transgenesis is relatively more straightforward
67 through the use of efficient transposon systems and direct zygote manipulation⁷. The transparent
68 larva is ideally amenable to imaging. The chemokine receptor dynamics have been visualized in
69 primordial germ cells and the lateral line primordium by expression of corresponding fusions with
70 fluorescent reporters⁸⁻¹⁰. Zebrafish larvae are equipped with mature neutrophils that have highly
71 conserved genetic and cellular properties with respect to mammalian neutrophils. Subcellular
72 signaling dynamics such as cytoskeletal dynamics and polarity regulators have been visualized in
73 these cells by the generation of corresponding transgenic lines¹¹⁻¹³. Recently, we visualized and
74 functionally analyzed chemokine receptor dynamics in neutrophils during the course of
75 inflammatory responses to tissue damage¹⁴. Here, we describe the generation of transgenic
76 reporter lines for chemokine signaling in neutrophils, preparation of embryos for live imaging, a
77 wound assay for studying neutrophil signaling and the protocol for acquisition and analysis of
78 images. We also provide a side-protocol to test chemokine receptor responses to candidate
79 ligands, which is useful when trying to establish ligand recognition patterns in uncharacterized
80 receptors. These techniques can be used in combination with further genetic manipulations, such
81 as inhibition of endogenous chemokine expression or generation of mutant receptors with
82 altered ligand-induced trafficking, to interrogate how specific signaling dynamics affect leukocyte
83 behavior in vivo. The transgenic lines expressing fluorescently tagged chemokine receptors can
84 also be used as reporters for endogenous chemokine gradients, which are otherwise difficult to
85 detect by direct antibody staining. The described methodology provides scope for expanding the
86 generation of reporters to other immuno-signaling receptors.

87
88 **PROTOCOL:**

89

90 NOTE: All zebrafish were kept according to the ARRIVE guidelines and UK Home Office
91 regulations, UK Animals (Scientific Procedures) Act 1986.

92

93 **1. Generation of transgenic reporter zebrafish larvae for imaging receptor trafficking in**
94 **leukocytes**

95

96 1.1. Generate Tol2-based construct for tissue specific expression of the fluorescently tagged
97 receptor of interest. For neutrophils, use promoter sequences from the lysozyme C¹⁵ and
98 myeloperoxidase gene¹⁶. The construct can be designed as a fusion with a single fluorescent
99 protein (e.g. GFP), a tandem fluorescent timer (e.g. a fast-folding GFP and a slower maturing
100 tagRFP^{8, 14, 17}) or a bicistronic expression of reporter GFP and a control membrane marker⁹ (see
101 **Discussion** for considerations when choosing the approach).

102

103 NOTE: This construct does not recapitulate endogenous levels of receptor expression but is useful
104 for obtaining high level of receptor expression in the cell type of interest. Consult the literature
105 on similar receptors^{3, 5, 6, 8-10, 14} to decide on the position of the fluorescent tag.

106

107 1.2. Set up a tank containing wild type adult males and females following standard husbandry
108 practices¹⁸, separated by a barrier the day before egg spawning.

109

110 1.3. On the day of egg spawning, prepare transgenesis mixture for microinjection containing
111 12.5 ng/μL of Tol2 DNA construct and 17.5 ng/μL of transposase mRNA⁷. Lift barriers from fish
112 tanks shortly after the lights come in the morning (this may vary in different fish facilities) and
113 collect eggs within 15 min for mRNA injection.

114

115 NOTE: Ensure the DNA solution is RNase free to avoid degradation of the transposase mRNA in
116 the mixture. An option to circumvent this is to inject eggs with separate solutions of Tol2
117 construct and transposase.

118

119 1.4. Follow standard protocols for transgenesis and microinjection of zebrafish eggs¹⁹.

120

121 1.5. Inject 1 nL of the solution into the cell of one-cell stage embryos.

122

123 NOTE: In our experience, the expression results are more consistent when injecting inside the
124 cell and discarding the injections that may not be clearly inside the cell. We aim for one-cell stage
125 embryos because of the variability of volume injection per cell when injecting 2-16 cell stage
126 embryos. An option would be to separate the one-cell stage injections from batches of later
127 injections, in case these have different efficacies.

128

129 1.6. Check the injected embryos later in the day and remove unfertilized or dead+ eggs to
130 keep the clutch healthy.

131

132 1.7. At 3 days post-fertilization (dpf), screen larvae under a fluorescent microscope. The

133 marker will be visible in neutrophils, particularly in the caudal hematopoietic tissue (CHT), which
134 is rich in these cells.

135
136 NOTE: The percentage of cells labeled varies with different constructs, but usually 20-60% of
137 neutrophils are expected to express the construct. Lower percentages usually predict more
138 screening at the adult stage. It is a good practice to also verify correct localization of the receptor
139 at the membrane, with a higher-resolution imaging approach, in a sample of these embryos
140 before growing the fish.

141
142 1.8. Grow positive larvae following standard husbandry practices²⁰. These represent the F0
143 generation.

144
145 1.9. At 3 months of age, screen F0 fish for founders. Cross individual fish with a non-transgenic
146 wild type and screen their offspring at 3 dpf for the expression of the receptor by viewing under
147 the dissecting scope. Depending on the transgenesis success, which varies with each construct,
148 observe a percentage of positive offspring in a subset of the crosses.

149
150 NOTE: For good transgenesis, about a third to a half of adults will give positive offspring. The
151 percentage of offspring that is positive in a clutch varies with the copy number of transgenes
152 inserted and, can be between 10-60%. It is helpful to keep track of mendelian ratios within the
153 clutches to identify single insertion transgenics (these are more easily identified in F2 clutches by
154 looking for a 50% ratio of positive larvae)²⁰.

155
156 1.10. Grow the positive offspring, which represent the F1 generation.

157
158 1.11. At 3 months of age, screen F1 adults in the same way to establish stable F2 transgenic
159 line.

160
161 1.12. Perform experiments on F2 larvae after validating the neutrophil-specific expression of
162 the transgene.

163
164 NOTE: During the transgenesis, one may observe varying levels of receptor expression and it is
165 advisable to keep different transgenic clutches to obtain the most appropriate expression level
166 for the biological questions. Initial results may be obtained in F0 or F1 larvae.

167 168 **2. Collecting zebrafish embryos for assessing leukocyte wound responses**

169
170 2.1. After having established a stable transgenic reporter line, set up an cross between adult
171 and female transgenic fish and collect eggs the next morning.

172
173 2.2. Grow embryos at 28.5 °C in E3 medium (or egg water¹⁸).

174 2.3. Optionally, at 24 hpf, incubate embryos in a centrifuge tube containing 50 mL of E3
175 medium supplemented with 0.003% bleach for 5 min. Subsequently rinse 3 times in E3 medium
176 by letting the tube stand for a couple of minutes to allow the embryos to settle in the bottom

177 and then decanting and replacing the medium.

178

179 NOTE: This provides a level of control on the infection exposure of the larvae, which may affect
180 the behavior of leukocytes during wounding.

181

182 2.4. After bleaching, keep embryos in E3 medium supplemented with 0.003% of 1-phenyl-2-
183 thiourea to prevent melanin synthesis. Methylene blue, which is often used to prevent fungal
184 infections, is not added here, to minimize tissue autofluorescence.

185

186 2.5. Allow larvae to hatch naturally and use at 3 dpf when neutrophils are abundant²¹.

187

188 **3. Ventral fin wounding of larvae**

189

190 3.1. Prepare larvae for wounding. Use larvae at 2.5-3.5 dpf, when abundant neutrophils are
191 observed. Transfer larvae to E3 medium supplemented with 160-200 mg/L tricaine MS222.

192

193 NOTE: Concentrated solutions of tricaine should be prepared and frozen in aliquots in advance
194 and thawed on the day.

195

196 3.2. Leave the larvae in E3+tricaine medium for 15 min to ensure they are anaesthetized.
197 Check their responses by gently touching with a small paintbrush or similar tool.

198

199 3.3. Select larvae with transgenic receptor expression under a fluorescent dissecting scope.

200

201 3.4. Transfer larvae to a 120 mm Petri dish in E3 + tricaine for wounding. Using a sterile scalpel
202 cut the ventral fin of the larva, while observing under the dissecting scope (**Figure 1**).

203

204 NOTE: The idea is to perform a deep enough cut to cause substantial neutrophil recruitment but
205 without cutting the vessels of the CHT. The cut is made perpendicular to the CHT axis such that
206 the incision nearly reaches the vessels of the CHT. This takes some practice and should first be
207 performed with supervision on larvae that are not generated for this purpose (e.g., excess larvae
208 from another experiment).

209

210 **4. Preparation of larvae for live imaging**

211

212 4.1. Dissolve low melting point (LMP) agarose in E3 medium by heating to obtain a liquid 2%
213 agarose solution.

214

215 4.2. Allow this solution to cool down to 60°C.

216

217 NOTE: Keep a flask or tube with agarose in an incubator at 60 °C to avoid the agarose setting
218 between the mounting of different larvae.

219

220 4.3. Pipette 0.5 mL of the liquid LMP + E3 in a glass bottom dish for microscopy imaging.

221
222 4.4. Pipette a wounded, anesthetised zebrafish larva along with 0.5 mL of E3 + 2x Tricaine in
223 the glass bottom dish.

224
225 4.5. Gently mix the two solutions to obtain a 1% LMP/1x Tricaine agarose/E3 solution,
226 avoiding generation of bubbles. Orient the embryo laterally and gently push down so that the
227 caudal part of the fish is as close as possible to the glass.

228
229 NOTE: The tissue to be imaged must be as close as possible to the glass bottom when imaging
230 with an inverted microscope. The setting of orientation for the larva must be quick so that the
231 agarose does not set before the larva is positioned.

232
233 4.6. Let the agarose solution cool down and solidify for 5-10 min. Test whether the agarose is
234 set by gently touching the agarose gel with a small paint brush or tip.

235
236 4.7. Once the agarose is solid, add 2 mL of E3 supplemented with 0.2 mg/mL of tricaine to the
237 imaging plate.

238
239 **5. Live confocal imaging**

240
241 NOTE: Image embryos on a spinning disk confocal microscope or equivalent (Figure 2). A laser
242 scanning microscope can also be used but the temporal resolution of the dynamics will be more
243 limiting. Prepare the imaging settings before bringing the wounded larva, so the response can be
244 imaged as quickly as possible after wounding. Neutrophils arrive to the wound within 5 min and
245 receptors in the first arriving cells may internalize within this time frame. With practice it is
246 possible to image as early as 15 min post-wounding.

247
248 5.1. Turn on the microscope: laser, camera and computer as per manufacturer instructions.

249
250 5.2. Use acquisition software to set up the imaging settings. Choose lasers for the appropriate
251 fluorophores and approximate exposure times based on previous experiments (acquire GFP with
252 488 nm and tagRFP with 561nm laser).

253
254 5.3. Transfer the plate with the mounted embryo, as soon as possible after agarose sets, onto
255 the confocal imaging spinning disc platform.

256
257 5.4. Use the microscope eye piece to find the fish in the dish using the stage joystick.

258
259 5.5. Focus on the wound area, using the focusing knob.

260
261 NOTE: To find the area of interest it may be easier to use a low magnification air objective (10x).

262
263 5.6. Select the field to image around the wound. Use a 30x/40x objective with high numerical
264 aperture to obtain sufficient resolution.

265
266 5.7. Use the software buttons to adjust the exposure time so that the fluorescent marker can
267 be seen with good contrast but without saturating the signal.

268
269 NOTE: The exposure time must be as low as possible to minimize fluorescent exposure and
270 maximize temporal resolution in the time-lapse. The laser power depends on the condition of
271 the laser but needs to be adjusted to a level that permits low enough exposure time for dynamic
272 imaging.

273
274 5.8. Use the software buttons to select the volume to image as a z-stack

275
276 5.9. Set up a time lapse every 30 s for the desired duration.

277
278 NOTE: For sterile ventral fin wounds, the maximum recruitment is observed by 2-3 h.

279
280 5.10. Before launching the time-lapse, take a bright field snapshot to document the field of
281 view. If possible, acquire bright field within the time-lapse movie.

282 283 **6. Quantification of receptor internalization in zebrafish neutrophils**

284
285 6.1. Record the time-interval of image acquisition and the pixel size of the image. Keep a
286 record of how many minutes post-wounding the imaging started.

287
288 6.2. Open the image datasets using Fiji by dragging the image onto the software interface,
289 select a representative frame of interest for each dataset using the time slider, e.g. at 1-1.5 h
290 post-wounding, and save it.

291
292 6.3. Proceed with MATLAB to process the image dataset.

293
294 6.4. Create a new script and include functions for image reading (line 6 in script called
295 'select_neutrophils.m' for centroid definition in Supplementary File 1), opening (line 11 in
296 Supplementary File 1) and manual selection of points on the image (line 12 in Supplementary File
297 1).

298
299 6.5. Open the frame of interest by running this script (Supplementary file 1), identify the
300 neutrophils to analyze by visual inspection, click on them and record an estimation of their
301 centroids, both in the ventral fin wound and in the CHT.

302
303 NOTE: The non-mobilized neutrophils in the CHT serve as an internal reference for neutrophils
304 whose receptor distribution remains constant. This allows normalization of contrast values of
305 cells at the wound to an internal reference.

306
307 6.6. Proceed with segmentation of the neutrophils in each frame using active contours
308 technique²² as described in steps below.

309
310 6.7. Create a function to include the metadata required for segmentation by active contours
311 (i.e. number of iterations, bias of contour, estimated centroid etc)²² (see 'wound_data.m' in
312 Supplementary file 2).
313
314 6.8. Create a script that calls the function 'wound_data.m' to input the necessary information
315 for segmentation of each neutrophil (line 28 in script called 'calc_contrast.m' in Supplementary
316 file 3).
317
318 6.9. Include in the script commands for image reading (line 32 in Supplementary file 3).
319
320 6.10. Add the generation of a black image (i.e. image where pixel values are zeros) with an
321 equal size to the input image (line 44 in Supplementary file 3) and the definition of a square of
322 10 × 10 pixels around the centroid of each neutrophil (line 45 in Supplementary file 3).
323
324 6.11. Include the neutrophil segmentation using active contours (lines 48-49 in Supplementary
325 file 3) and the removal of small false detected objects (line 52 in Supplementary file 3).
326
327 NOTE: The initial segmentation contour is the square around the centroid, which evolves by
328 active contour technique based on the pixel intensities, the number of iterations and the bias of
329 contour. The result of segmentation is a binary mask where all pixels have value 0 apart from the
330 neutrophil area whose pixels have value 1.
331
332 6.12. Include the multiplication of the segmented binary image with the original one to get the
333 pixel intensities of the neutrophil only, with the rest of the image being not-a-number, so it does
334 not contribute to calculations (lines 56-57 in Supplementary file 3).
335
336 6.13. Add the calculation of the gray-level co-occurrence matrix for each neutrophil (GLCM)¹⁴,
337 ²³ (line 61 in Supplementary file 3).
338
339 NOTE: GLCM is another representation of the image showing relative position of pixels in terms
340 of pixel intensity.
341
342 6.14. Include the calculation of contrast of the neutrophil based on the GLCM (lines 62,65 in
343 Supplementary file 3). NOTE: The contrast metric measures differences in intensity between
344 neighboring pixels. Pixels are compared with pixels certain distance apart, which can be adjusted
345 empirically based on the size of local peaks in intensity. As an indication, for our images, with a
346 pixel size of 0.389 μm, when the receptor showed vesicular distribution each bright dot was in
347 the range of 5 pixels. We therefore compared intensities in pixels spaced 5 pixels apart.
348 6.15. Add commands to save the values separately for individual neutrophils in the ventral fin
349 (line 68 in Supplementary file 3).
350
351 6.16. Include the calculation of the mean neutrophil contrast value from all CHT neutrophils
352 the same way as for neutrophils at the wound (lines 72-119 in Supplementary file 3). For CHT

353 neutrophils, call the function 'cht_data.m' (line 77 in Supplementary file 4).

354

355 6.17. Include the normalization of the contrast value of individual neutrophils at the wound to
356 the mean contrast of CHT neutrophils calculated above in step 6.16 (i.e. division) (line 122 in
357 Supplementary file 3). NOTE: This gives a normalized contrast that reflects how 'dotty' the
358 appearance of receptor is in individual responding cells relative to control non-responding cells
359 (Figure 3 and 4).

360

361 6.18. Run the script (Supplementary file 3) by clicking the run symbol in the software.

362

363 6.19. Repeat all steps for different conditions.

364

365 6.20. Use statistical software (see **Table of Materials**) to import the results for the different
366 conditions by creating a column table, plot the results and perform statistical test to check
367 significance of difference between the mean values.

368

369 NOTE: The codes for the analysis can also be found in GitHub at
370 <https://github.com/LeukocyteMotionAndDynamics/ReceptorTraffic>

371

372 **7. Chemokine response assays in early embryos**

373

374 NOTE: This is an optional side experiment that allows testing of receptor distribution changes in
375 response to a candidate chemokine and is independent from the experiments described above
376 concerning neutrophil expression of the receptor constructs. Differences in ligand-induced
377 trafficking between receptors are difficult to establish with this technique as the ligand levels are
378 saturating¹⁴. However, if one sees ligand-internalization of a receptor in this system, this can be
379 an indication that the ligand is recognized by the receptor in instances where the ligand identity
380 is unclear. This is useful, because expression of chemokine receptors in established cell lines such
381 as HEK293T cells¹⁴ can be cumbersome.

382

383 7.1. Set up a cross of wild type fish (e.g., AB) and collect eggs the next morning shortly after
384 lifting the separators (as described above).

385

386 7.2. Inject 100 pg of fluorescently tagged receptor mRNA (e.g., Cxcr1-FT), together with 100
387 pg of mRNA for a membrane marker (e.g., membrane CFP). Include in the mixture varying doses
388 of mRNA for chemokine ligand.

389

390 NOTE: As an indication 150 pg Cxcl8a mRNA gave prominent internalisation of fluorescent Cxcr1-
391 FT (**Figure 5**).

392

393 7.3. Rinse embryos with E3 medium and incubate at 28°C.

394

395 7.4. At about 7 hpf, test expression of the mRNA on a fluorescent dissecting scope and select
396 the embryos to image.

397
398 7.5. Prepare 0.8 % LMP agarose in advance and keep in glass tube in a heatblock at 60 °C. Use
399 a glass pipette to manipulate the embryos. Gently dechorionate embryos using a pair of forceps
400 in each hand.

401
402 7.6. Aspirate an individual dechorionated embryo with the glass pipette ensuring no bubbles
403 are at the tip. Gently release the embryo into the tube of agarose allowing it to sink into the tube.
404

405 7.7. Aspirate the embryo from the agarose tube, collecting some liquid agarose along the way.
406 Gently release embryo onto the center of a glass-bottomed imaging dish. Quickly rotate embryo
407 so that the animal pole is facing the bottom of the dish (this side has to be closest to the objective
408 when using an inverted microscope).

409
410 NOTE: One may need to readjust the orientation of embryos while the agarose is still setting.

411
412 7.8. After the agarose is set, supplement with 2 mL of E3 medium.

413
414 NOTE: The embryos at this stage are very fragile in comparison to larvae and it takes some
415 practice to dechorionate and mount. It is important to aspirate and release as gently as possible,
416 to avoid embryo rupture.

417
418 7.9. Repeat the process aiming to load 3-5 embryos per dish.

419
420 7.10. Image embryos on an inverted confocal microscope (see **Table of Materials**). Use a
421 40×/1.3 NA oil objective to obtain high enough resolution. Visualize mCFP, sfGFP, and tagRFP
422 with 405, 488, and 552 nm, respectively, on the Leica scope. Adjust filters and settings to have
423 high contrast while avoiding saturation and minimize leak through between the channels.

424
425 7.11. Repeat the mounting and imaging for different conditions.

426 427 **REPRESENTATIVE RESULTS:**

428 Ventral fin wounding is followed by rapid neutrophil mobilization from the CHT into the ventral
429 fin and clustering at the wound margin, within 30-60 min (**Figure 1**). We visualized the
430 distribution of two chemokine receptors, Cxcr1 and Cxcr2, which are expressed by zebrafish
431 neutrophils²⁴ and recognize Cxcl8a and Cxcl8b¹⁴, using spinning-disk confocal microscopy. We
432 generated two corresponding transgenic lines, Tg(*lyz:Cxcr1-FT*) and Tg(*lyz:Cxcr2-FT*), in which
433 neutrophils express a fluorescent timer (FT) construct of the receptor, i.e. a fusion with a tandem
434 of sfGFP and tagRFP (**Figure 2** and reference¹⁴). The use of the two fluorophores was intended to
435 allow monitoring of a broad range of receptor fates and provide estimates of protein turnover
436 time at the plasma membrane, as newly synthesized receptors would fluoresce in green and
437 progressively become red as they age^{8, 14}. However, these receptors were found to have fast
438 constitutive turnover at the neutrophil plasma membrane and that the residence time was
439 shorter than the maturation time of tagRFP, with sfGFP showing membrane localisation and
440 tagRFP showing vesicular localization at steady state (**Supplementary Video 1** and ref¹⁴).

441 Therefore, we focused on the distribution of sfGFP to monitor ligand-induced internalization at
442 sites of tissue damage. The pattern of receptor distribution was quantified using the contrast
443 metric, which reports differences in intensity between neighboring pixels. The rationale is that
444 when the receptor distribution is membranous and smooth, the contrast value is low. When the
445 receptor distribution is vesicular and more punctate, then the contrast value is high (**Figure 3**).

446
447 An alternative method is to quantify the ratio of receptor levels (sfGFP intensity) over the levels
448 of a control membrane marker e.g. membrane CFP (mCFP) (**Figure 3**). Both methods could detect
449 receptor internalization, as indicated by more vesicular receptor distribution pattern globally in
450 the cell (higher contrast value) or lower receptor levels at the membrane (lower sfGFP/mCFP
451 ratio). However, the contrast metric could also detect receptor internalization in neutrophil
452 clusters at the wound, in which membrane segmentation was less accurate and not applicable
453 (**Figure 3**). Using this metric, we were able to quantify visible differences between Cxcr1 and
454 Cxcr2 trafficking in neutrophils at wounds (**Figure 4** and **Supplementary Video 2**). Cxcr1-FT
455 internalized in cells located at the wound whereas Cxcr2-FT remained membranous in
456 neutrophils at the wound (**Figure 4A-C**, **Supplementary Video 2** and **Supplementary Video 3**).
457 Suppression of Cxcl8a and Cxcl8b, through morpholino treatment, differentially affected Cxcr1-
458 FT internalization at wounds (**Figure 4C,D**). To further validate that Cxcr1-FT responds to Cxcl8a,
459 we performed chemokine response assays in early embryos. We found that Cxcr1-FT markedly
460 internalized in embryos in which Cxcl8a was co-expressed (**Figure 5**). Altogether these results
461 indicate that the described methods can be deployed to measure chemokine-induced receptor
462 internalization in neutrophils and establish the identity of the ligand mediating these effects.

463 464 **FIGURE AND TABLE LEGENDS:**

465
466 **Figure 1: Neutrophil migration to ventral fin wounds.** (A) (Left) Cartoon of 3 dpf larva showing
467 the location of the caudal hematopoietic tissue (CHT), the venous circulation (VC, blue), the
468 ventral fin (VF) and the wound site. (Right) Cartoon depicting the area of the wound (W) with
469 neutrophils getting mobilized from the CHT and clustering at the wound. The caudal vein plexus
470 (CVP) of the CHT tissue is drawn in blue. (B) Bright field image (left) and confocal projection
471 (right) showing the ventral fin wound and the distribution of neutrophils in Tg(*mpx*:GFP) larvae
472 at 2 h post-wounding. Dashed lines show VF and CHT outlines. Scale bar = 25 μ m. Cartoon and
473 fluorescent image modified from ref.¹⁴ (<http://creativecommons.org/licenses/by/4.0/>).

474
475 **Figure 2: Live imaging of chemokine receptor trafficking in neutrophils.** (A) Constructs used for
476 neutrophil-specific transgenic expression of Cxcr1-FT (Fluorescent Timer) and Cxcr2-FT. Confocal
477 projections of neutrophils in the head of a 3 dpf transgenic larva (Tg(*lyz*:Cxcr1-FT), top;
478 Tg(*lyz*:Cxcr2-FT), bottom) showing tRFP (magenta) and sfGFP (green) channels. Scale bar = 20
479 μ m. (B) Anatomical scheme of 3 dpf larva as in Figure 1A. Below the larva are schemes depicting
480 the area of the wound (W) with neutrophils getting mobilized from the CHT (top) or performing
481 chemotaxis upon entering the ventral fin (bottom). Dashed square indicates area imaged in
482 snapshots on the right. (C) Neutrophils in Tg(*lyz*:Cxcr1-FT) larvae (sfGFP is shown) upon
483 mobilization from the CHT (top panels) or chemotaxis towards the wound (bottom panels).
484 Arrows show the same cells over time. Time points on the right image are minutes elapsed after

485 image on the left. Scale bar = 10 μm . **(D)** Schematic representation of experimental approach for
486 live imaging of chemokine receptor trafficking. Panels A-C modified from ref.¹⁴
487 (<http://creativecommons.org/licenses/by/4.0/>).

488
489 **Figure 3: Quantification examples of receptor dynamics.** Single (blue) or clustered neutrophils
490 (green) at wounds or non-mobilized neutrophils in the CHT (red, orange) were segmented and
491 analyzed by different methods to compare results. The same example cells shown were analyzed
492 with two methods to relate what is seen in the image with the range of values extracted. **(A)** The
493 surface of the selected, example cells were segmented based on contour definition in the sfGFP
494 channel. **(B)** Contrast was computed from the example cells shown in A. **(C)** The membrane of
495 the selected, example cells was segmented based on contour definition in the CFP channel.
496 Ratiometric analysis of sfGFP/CFP followed. **(D)** The ratio of sfGFP/CFP was computed on the
497 example cells shown in c. Error bars represent S.E.M. from individual cells, in cases of $n > 1$, values
498 here were not used for statistical analysis but merely to exemplify measurements obtained with
499 the different quantification methods. Scale bar = 10 μm . Figure modified from ref.¹⁴
500 (<http://creativecommons.org/licenses/by/4.0/>).

501
502 **Figure 4: Differential dynamics of Cxcr1 and Cxcr2 in response to wounding.** **(A)** Confocal
503 projection of neutrophils in Tg(*lyz:Cxcr1-FT*) or Tg(*lyz:Cxcr2-FT*) larvae at the wound at 80 min
504 post-wounding (sf GFP channel shown)). Scale bar = 10 μm . mpw = minutes post-wounding. **(B)**
505 Magnified Cxcr1-FT neutrophil (left) and Cxcr2-FT (right) at the wound. Green receptor is shown
506 in grey. Scale bar = 5 μm . **(C)** Normalized contrast (contrast per individual neutrophil normalized
507 to the mean contrast of non-mobilized cells in the CHT). *cxcl8a* refers to injection of a splice-
508 blocking together with a translation-blocking morpholino for *cxcl8a*. *cxcl8b* refers to injection
509 with a splice-blocking morpholino for *cxcl8b*. For Tg(*lyz:Cxcr1-FT*): $n=24$ cells (CHT), $n=47$ cells
510 (wound) from 8 larvae. For Tg(*lyz:Cxcr1-FT*) with morpholinos: $n=28$ cells (Cxcl8a-MO) from 5
511 larvae, $n=16$ cells (Cxcl8b-MO) from 5 larvae. For Tg(*lyz:Cxcr2-FT*): $n=10$ cells (CHT) and $n=20$ cells
512 (wound) from 3 larvae. Data were pooled from independent larvae acquired in 1-5 imaging
513 sessions. Kruskal-Wallis test with Dunn's multiple comparisons test for Tg(*lyz:Cxcr1-FT*), two-
514 tailed unpaired Mann-Whitney test for Tg(*lyz:Cxcr2-FT*). **(D)** Confocal projection of neutrophils in
515 Tg(*lyz:Cxcr1-FT*) transgenic larvae treated with *cxcl8a* morpholino (MO) (left) and *cxcl8b* MO
516 (right) responding to fin wounds (sfGFP channel shown in green). Snapshot taken at timepoints
517 of equivalent neutrophil accumulation (85 mpw in left image and 45 mpw in right image). Scale
518 bar = 10 μm . Figure modified from ref.¹⁴ (<http://creativecommons.org/licenses/by/4.0/>).

519
520 **Figure 5: Chemokine response assay in early embryos.** Laser-scanning confocal slices of
521 gastrulating embryos showing expression and distribution of Cxcr1-FT. 100 pg of Cxcr1-FT mRNA
522 was injected into one cell-stage eggs with or without 150 pg Cxcl8a mRNA. Green and red
523 receptors are shown in separate channels. Control membrane CFP marker (mCFP) is shown in the
524 cyan channel. Scale bar = 20 μm . Figure modified from ref.¹⁴
525 (<http://creativecommons.org/licenses/by/4.0/>).

526
527 **Supplementary Movie 1:** Transgenic neutrophils in the head of a Tg(*lyz:Cxcr1-FT*) (left) and
528 Tg(*lyz:Cxcr2-FT*) (right) larva at 3 dpf. sfGFP(green), tagRFP (magenta). Frame interval is 30 sec

529 and frame rate is 5 fps. Scale bar = 20 μm . Video originates from ref.¹⁴
530 (<http://creativecommons.org/licenses/by/4.0/>).

531
532 **Supplementary Movie 2:** Neutrophils in Tg(*lyz:Cxcr1*-FT) (left) and Tg(*lyz:Cxcr2*-FT) (right)
533 transgenic larvae responding to fin wounds. Movie starts within 10 mpw and lasts 60 min. sfGFP
534 (green), tagRFP (magenta). Frame interval is 30 sec and frame rate is 10 fps. CHT = caudal
535 hematopoietic tissue. VF = ventral fin. Scale bar = 25 μm . Video originates from ref.¹⁴
536 (<http://creativecommons.org/licenses/by/4.0/>).

537
538
539 **Supplementary Movie 3.** Additional examples of neutrophils from a wounded Tg(*lyz:Cxcr1*-
540 FT) transgenic larva (different larva to that shown in Video 2), acquired at higher resolution,
541 showing receptor internalization (sfGFP channel shown in green) upon mobilization in the
542 CHT or upon entry and chemotaxis in the ventral fin. Frame interval is 30 sec and frame rate is
543 fps. Scale bar = 10 μm . Video originates from ref.¹⁴ (<http://creativecommons.org/licenses/by/4.0/>).

544 2

545
546 **DISCUSSION:**

547 The method described allows live imaging of receptor dynamics in response to endogenous
548 ligands in situ during an inflammatory response to tissue damage. The use of Cxcr1/Cxcr2
549 neutrophil reporters could be expanded to other physiological settings, such as infection, tumor
550 models or other types of tissue damage^{14, 25–27}. In addition, transgenic rescue lines, in which the
551 endogenous receptor is suppressed and rescued by an exogenous mutant receptor, could provide
552 useful tools to dissect the importance of specific neutrophil migration patterns in immune
553 responses. For example, Cxcr1 receptor mutants that have impaired desensitization cause more
554 prominent neutrophil clustering at inflammatory sites¹⁴. This gain of function phenotype could
555 be used to understand the role of neutrophil congregation in different physiological processes,
556 e.g., wound repair, infectious disease, or tumor evolution, and complement receptor
557 knockdown/knockout experiments. The methodology also provides a basis to expand the range
558 of available reporters. The choice of fluorescent reporter is important to consider and depends
559 on the biological question. We found that the constitutive turnover of these chemokine receptors
560 in neutrophils was high, in comparison to epithelial cells, and that reporters with fast maturation
561 (e.g., sfGFP) were required to report membrane levels at steady state and resolve differences
562 upon neutrophil stimulation^{8, 14}. Thus, membrane ratios of sfGFP/tagRFP are not applicable for
563 measuring ligand-induced internalization in this cell type, but the pattern of tagRFP allows
564 tracking of the intracellular fates of the receptor, which could be useful in some studies. We also
565 found that the more concentrated intracellular signal of tagRFP is useful for screening individual
566 larvae. An alternative approach for measuring receptor levels at the plasma membrane would be
567 to co-express a fluorescent membrane marker in neutrophils either in the same transgene⁹ or in
568 an independent transgene¹⁴. In the former scenario the transgene would provide an additional
569 means for screening the fish and expression levels would be comparable between the marker
570 and the receptor. The latter approach would be more modular, in that a zebrafish line with a
571 receptor reporter could be combined with different reporter lines. In either case, it is worth
572 noting that membrane quantification of the receptor levels is challenging in clustered neutrophils

573 (see below). Finally, we note that a possible extension of this protocol would be to follow up the
574 live imaging by immunohistochemistry for more detailed localization analyses.

575
576 The Tol2 transgenesis system is well established⁷ and the lysozyme C promoter has been used
577 extensively for neutrophil expression^{11, 15}. The transgenesis approach is, therefore, relatively
578 straightforward and the expression level achieved with this promoter is high enough to provide
579 sufficient contrast for analysis of receptor dynamics. A possible limitation is that the expression
580 level does not recapitulate endogenous receptor expression levels. New CRISPR technologies
581 could be deployed to establish knock-in lines for receptors of particular interest²⁸. These
582 technologies are still cumbersome and may not guarantee the required expression levels for
583 subcellular imaging, but their successful development would be an important breakthrough for
584 understanding endogenous signaling dynamics. Functional validations are important for
585 interpreting data with transgenic receptor constructs. For example, ligand recognition assays can
586 be used to establish that the fluorescent fusion protein is functional and rescue of knockout
587 phenotypes could be used to establish that the transgenic neutrophil expression levels are
588 compatible with functionality¹⁴. Finally, a more direct way to validate the receptor fusion would
589 be to utilize an *in vitro* functional assay with labelled receptor alongside non-labelled versions¹⁴.

590
591 The quantification approach addresses specific difficulties in accurate membrane segmentation
592 in neutrophils *in vivo*. In cells of epithelial nature, quantification of receptor levels can be
593 executed automatically by normalizing membrane receptor levels to a control marker, which can
594 be expressed in tandem or separately⁹. Indeed, we have applied such an approach, when using
595 the ligand-recognition assay in gastrulating embryos¹⁴. However, neutrophils undergo complex,
596 rapid changes in cell shape *in vivo*, making the membrane segmentation difficult both in 2D and
597 3D¹⁴. This is even more challenging when neutrophils cluster, which occurs in many physiological
598 settings²⁹. The contrast metric overcomes this limitation as it does not require membrane
599 segmentation but instead reflects the overall state of receptor distribution in the cell
600 (membranous/smooth vs vesicular/dotty). It is important to note that contrast metric can be
601 affected by the overall contrast of the image, so normalization of individual cell values to an
602 internal reference is required to account for variability of signal in different embryos/samples.
603 For example, we used the mean cell contrast value of non-responsive neutrophils in the CHT (i.e.
604 neutrophils that remain stationary and do not migrate into the ventral fin)¹⁴. An additional
605 possibility would be to normalize with contrast values of a control marker in the same cell. This
606 would provide a solution when an internal reference of non-responding cells is not available and
607 may likely resolve finer quantitative differences in receptor dynamics between different
608 conditions.

609
610 The location of imaging is another variable to consider. The reason for choosing the ventral fin
611 wound here, as opposed to the more commonly used tail fin wound model^{16, 30}, is because the
612 site of wounding is nearby the site of neutrophil residence/migratory origin. This accelerates the
613 timeline of the assay, as it takes relatively little time for neutrophils to arrive. Additionally, it
614 provides the opportunity to capture cell behavior both at the migration origin (CHT) and the
615 target location of interest (wound). This is relevant here, because the spatial and temporal
616 resolution required for subcellular imaging is difficult to combine with a large field of view or

617 multi-position scanning. Thus, the ventral fin wound assay permits tracking of the evolution of
618 the migratory response from the migration origin and simultaneous capturing of unspecific
619 receptor fluctuations in cells that do not respond. As mentioned above, the latter is useful for
620 quantification purposes as it provides an internal reference for unspecific dynamics. In other
621 systems, it may not be possible to have such an internal reference, in which case the contrast
622 values of a co-expressed membrane marker would provide an alternative control.

623
624 In summary, we anticipate that the methodology is applicable to other systems and can be
625 deployed for a variety of purposes. For example, the same reporters could be utilized in other
626 inflammatory settings, such as infection settings or other disease models. The repertoire of
627 zebrafish receptor reporter lines could be expanded to other signalling receptors, to understand
628 signalling mechanisms or report ligand dynamics *in vivo*. The approach can be combined with
629 knockdown/knockout techniques to interrogate the mechanistic basis of observed dynamics. For
630 example, perturbation of ligand expression can indicate the ligand dependency for observed
631 receptor dynamics. In the future, we envisage that the system could be further refined to
632 incorporate knock-in insertion of reporters. Ultimately, findings using this methodology would
633 provide novel insights valuable beyond the zebrafish community, given the conservation of these
634 signaling receptors in mammals and the relative challenge of conducting these studies in larger
635 organisms.

636
637 **ACKNOWLEDGMENTS:**

638 We thank Christine Holt and Bill Harris for help with confocal microscopy. We thank Darren
639 Gilmour for the fluorescent timer backbone constructs and Anna Huttenlocher for the Tol2-Lyz
640 backbone vector. We thank Steve Renshaw for the Tg(*mpx*:GFP)ⁱ¹¹⁴ line. This work was supported
641 by the MRC (MR/L019523/1), the Wellcome Trust [204845/Z/16/Z]; Isaac Newton Trust
642 [12.21(a)i] and an Isaac Newton Trust grant 19.23(n). C. C was supported by an MRC DTP
643 studentship and partly by the Wellcome Trust [204845/Z/16/Z]; Isaac Newton Trust [12.21(a)i]
644 grant. H.W. was supported by an MRC DTP Studentship. H.P. was supported by a Wellcome Trust
645 PhD grant (105391/Z/14/Z) and partly by a Wellcome Trust [204845/Z/16/Z]; Isaac Newton Trust
646 [12.21(a)i] grant and the MRC (MR/L019523/1).

647
648 **DISCLOSURES:**

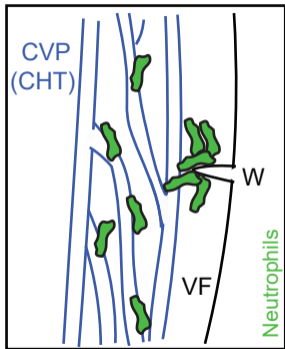
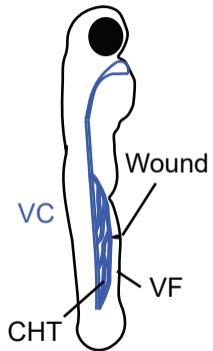
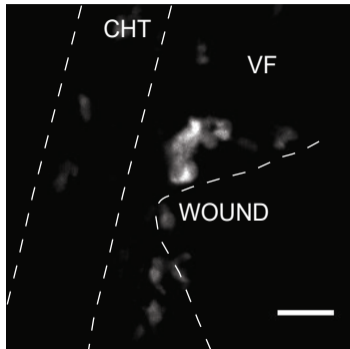
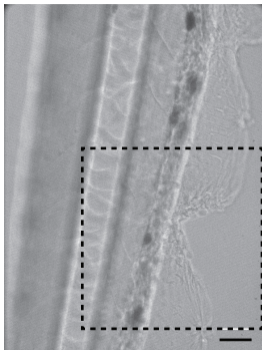
649 The authors declare no conflict of interest
650

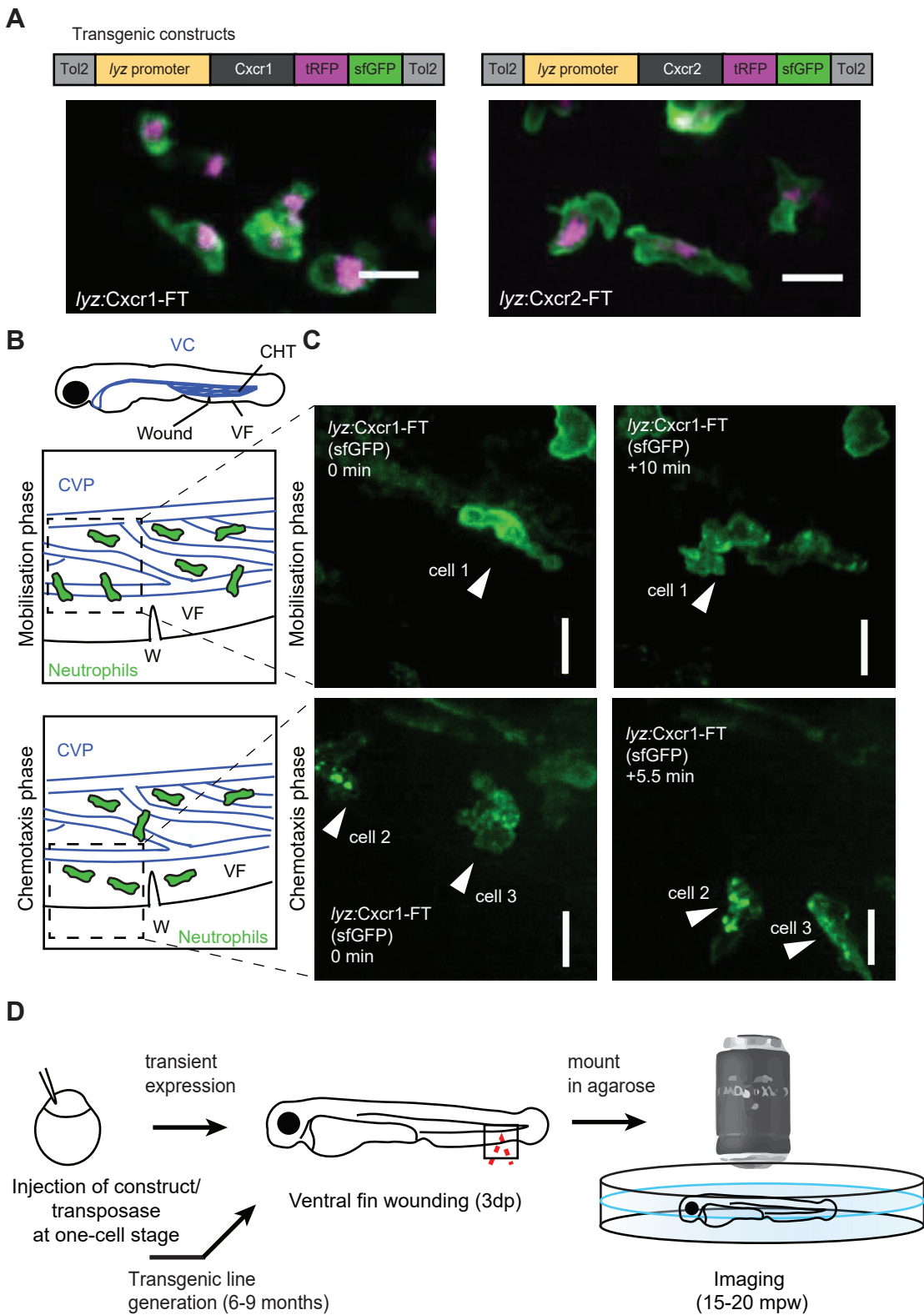
651 **REFERENCES:**

- 652 1. Rot, A., von Andrian, U.H. Chemokines in innate and adaptive host defense: basic
653 chemokines grammar for immune cells. *Annual Review of Immunology*. **22**, 891–928, doi:
654 10.1146/annurev.immunol.22.012703.104543 (2004).
- 655 2. Cotton, M., Claing, A. G protein-coupled receptors stimulation and the control of cell
656 migration. *Cellular Signalling*. **21** (7), 1045–1053, doi: 10.1016/j.cellsig.2009.02.008 (2009).
- 657 3. Liu, X. *et al.* Bidirectional regulation of neutrophil migration by mitogen-activated protein
658 kinases. *Nature Immunology*. **13** (5), 457–464, doi: 10.1038/ni.2258 (2012).

- 659 4. Wen, X., Jin, T., Xu, X. Imaging G Protein-coupled Receptor-mediated Chemotaxis and its
660 Signaling Events in Neutrophil-like HL60 Cells. *Journal of Visualized Experiments*. (115),
661 54511, doi: 10.3791/54511 (2016).
- 662 5. Arnon, T.I. *et al.* GRK2-dependent S1PR1 desensitization is required for lymphocytes to
663 overcome their attraction to blood. *Science (New York, N.Y.)*. **333** (6051), 1898–1903, doi:
664 10.1126/science.1208248 (2011).
- 665 6. Jung, H., Mithal, D.S., Park, J.E., Miller, R.J. Localized CCR2 Activation in the Bone Marrow
666 Niche Mobilizes Monocytes by Desensitizing CXCR4. *PLOS ONE*. **10** (6), e0128387, doi:
667 10.1371/journal.pone.0128387 (2015).
- 668 7. Kwan, K.M. *et al.* The Tol2kit: a multisite gateway-based construction kit for Tol2
669 transposon transgenesis constructs. *Developmental Dynamics: An Official Publication of the*
670 *American Association of Anatomists*. **236** (11), 3088–3099, doi: 10.1002/dvdy.21343 (2007).
- 671 8. Donà, E. *et al.* Directional tissue migration through a self-generated chemokine gradient.
672 *Nature*. **503** (7475), 285–289, doi: 10.1038/nature12635 (2013).
- 673 9. Venkiteswaran, G., Lewellis, S.W., Wang, J., Reynolds, E., Nicholson, C., Knaut, H.
674 Generation and dynamics of an endogenous, self-generated signaling gradient across a
675 migrating tissue. *Cell*. **155** (3), 674–687, doi: 10.1016/j.cell.2013.09.046 (2013).
- 676 10. Minina, S., Reichman-Fried, M., Raz, E. Control of receptor internalization, signaling level,
677 and precise arrival at the target in guided cell migration. *Current biology: CB*. **17** (13), 1164–
678 1172, doi: 10.1016/j.cub.2007.05.073 (2007).
- 679 11. Yoo, S.K., Lam, P.-Y., Eichelberg, M.R., Zasadil, L., Bement, W.M., Huttenlocher, A. The role
680 of microtubules in neutrophil polarity and migration in live zebrafish. *Journal of Cell Science*.
681 **125** (Pt 23), 5702–5710, doi: 10.1242/jcs.108324 (2012).
- 682 12. Yoo, S.K., Deng, Q., Cavnar, P.J., Wu, Y.I., Hahn, K.M., Huttenlocher, A. Differential
683 regulation of protrusion and polarity by PI3K during neutrophil motility in live zebrafish.
684 *Developmental Cell*. **18** (2), 226–236, doi: 10.1016/j.devcel.2009.11.015 (2010).
- 685 13. Buchan, K.D. *et al.* A transgenic zebrafish line for in vivo visualisation of neutrophil
686 myeloperoxidase. *PLOS ONE*. **14** (4), e0215592, doi: 10.1371/journal.pone.0215592 (2019).
- 687 14. Coombs, C. *et al.* Chemokine receptor trafficking coordinates neutrophil clustering and
688 dispersal at wounds in zebrafish. *Nature Communications*. **10** (1), 5166, doi:
689 10.1038/s41467-019-13107-3 (2019).
- 690 15. Hall, C., Flores, M.V., Storm, T., Crosier, K., Crosier, P. The zebrafish lysozyme C promoter
691 drives myeloid-specific expression in transgenic fish. *BMC developmental biology*. **7**, 42, doi:
692 10.1186/1471-213X-7-42 (2007).
- 693 16. Renshaw, S.A., Loynes, C.A., Trushell, D.M.I., Elworthy, S., Ingham, P.W., Whyte, M.K.B. A
694 transgenic zebrafish model of neutrophilic inflammation. *Blood*. **108** (13), 3976–3978, doi:
695 10.1182/blood-2006-05-024075 (2006).
- 696 17. Khmelinskii, A. *et al.* Tandem fluorescent protein timers for in vivo analysis of protein
697 dynamics. *Nature Biotechnology*. **30** (7), 708–714, doi: 10.1038/nbt.2281 (2012).
- 698 18. Westerfield M *The zebrafish book. A guide for the laboratory use of zebrafish (Brachydanio*
699 *rerio)*. Eugene, Oregon. University of Oregon Press, Eugene. (2007).
- 700 19. Rosen, J.N., Sweeney, M.F., Mably, J.D. Microinjection of Zebrafish Embryos to Analyze
701 Gene Function. *Journal of Visualized Experiments*. (25), 1115, doi: 10.3791/1115 (2009).

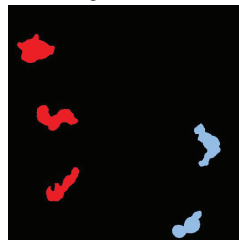
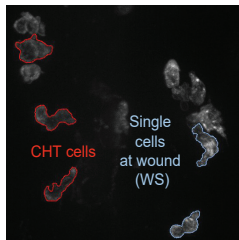
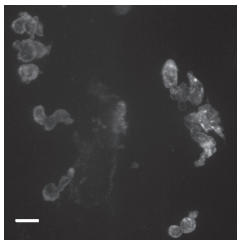
- 702 20. Detrich, H.W., Zon, L.I., Westerfield, M. *The Zebrafish: Genetics, Genomics and Informatics*.
703 at <<http://public.ebookcentral.proquest.com/choice/publicfullrecord.aspx?p=298293>>.
704 Elsevier. Burlington. (2004).
- 705 21. Le Guyader, D. *et al.* Origins and unconventional behavior of neutrophils in developing
706 zebrafish. *Blood*. **111** (1), 132–141, doi: 10.1182/blood-2007-06-095398 (2008).
- 707 22. Chan, T.F., Vese, L.A. Active contours without edges. *IEEE Trans Image Process*. **10** (2), 266–
708 277, doi: 10.1109/83.902291 (2001).
- 709 23. Haralick, R. M., Shanmugam, K. & Dinstein Textural Features for Image Classification. **SMC-3**
710 (6), 610–621 (1973).
- 711 24. Deng, Q., Sarris, M., Bennin, D.A., Green, J.M., Herbomel, P., Huttenlocher, A. Localized
712 bacterial infection induces systemic activation of neutrophils through Cxcr2 signaling in
713 zebrafish. *Journal of Leukocyte Biology*. **93** (5), 761–769, doi: 10.1189/jlb.1012534 (2013).
- 714 25. Torraca, V., Mostowy, S. Zebrafish Infection: From Pathogenesis to Cell Biology. *Trends in*
715 *Cell Biology*. **28** (2), 143–156, doi: 10.1016/j.tcb.2017.10.002 (2018).
- 716 26. Feng, Y., Santoriello, C., Mione, M., Hurlstone, A., Martin, P. Live imaging of innate immune
717 cell sensing of transformed cells in zebrafish larvae: parallels between tumor initiation and
718 wound inflammation. *PLoS biology*. **8** (12), e1000562, doi: 10.1371/journal.pbio.1000562
719 (2010).
- 720 27. Poplimont, H. *et al.* Neutrophil Swarming in Damaged Tissue Is Orchestrated by Connexins
721 and Cooperative Calcium Alarm Signals. *Current Biology*. S0960982220306692, doi:
722 10.1016/j.cub.2020.05.030 (2020).
- 723 28. Cornet, C., Di Donato, V., Terriente, J. Combining Zebrafish and CRISPR/Cas9: Toward a
724 More Efficient Drug Discovery Pipeline. *Frontiers in Pharmacology*. **9**, 703, doi:
725 10.3389/fphar.2018.00703 (2018).
- 726 29. Kienle, K., Lämmermann, T. Neutrophil swarming: an essential process of the neutrophil
727 tissue response. *Immunological Reviews*. **273** (1), 76–93, doi: 10.1111/imr.12458 (2016).
- 728 30. Lisse, T.S., Brochu, E.A., Rieger, S. Capturing Tissue Repair in Zebrafish Larvae with Time-
729 lapse Brightfield Stereomicroscopy. *Journal of Visualized Experiments*. (95), 52654, doi:
730 10.3791/52654 (2015).
- 731

A**B**

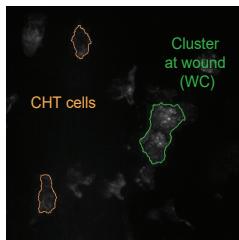
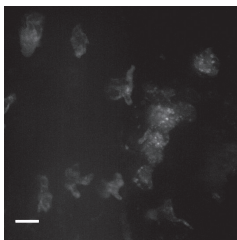
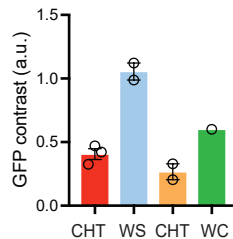


A

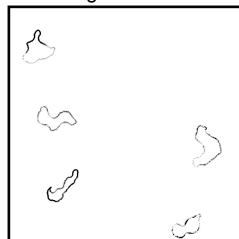
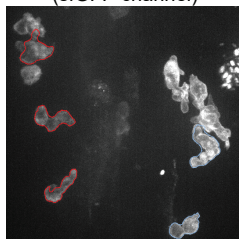
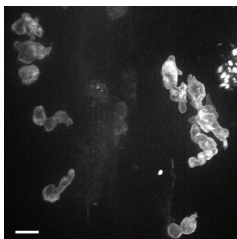
sfGFP channel

cell contour definition
on selected cellscontour-based surface
segmentation*lyz:Cxcr1-FT|lyz:mCFP*
wounded larva 1

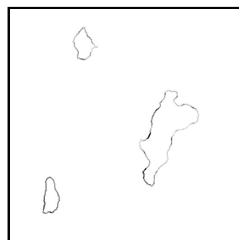
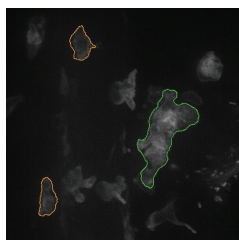
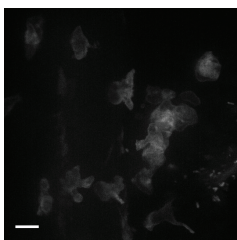
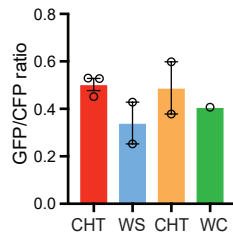
METHOD 1:
Surface
segmentation
followed by
contrast
computation
(chosen)

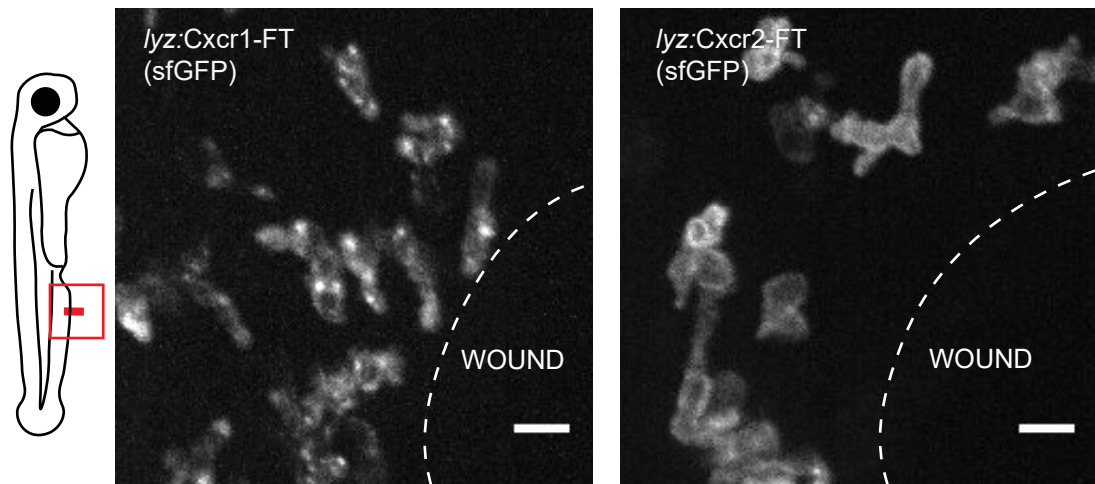
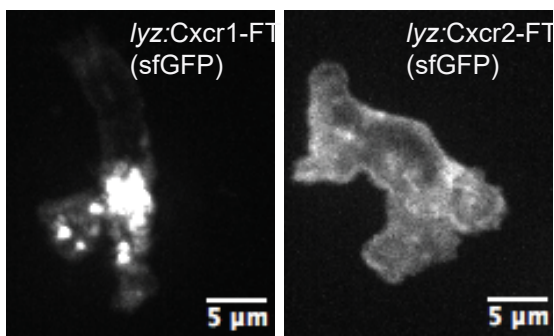
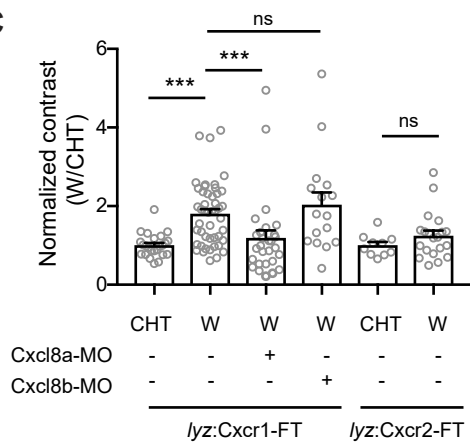
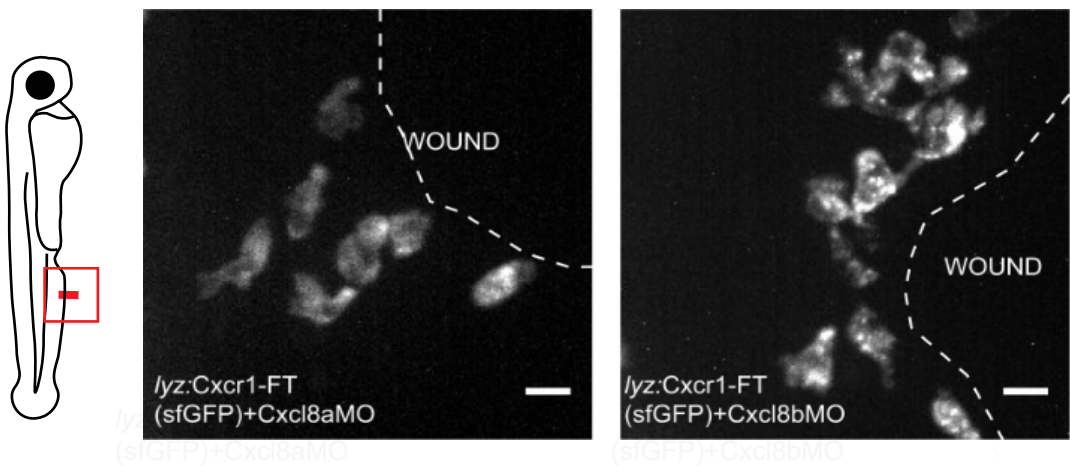
lyz:Cxcr1-FT|lyz:mCFP
wounded larva 2**B****C**

CFP channel

cell contour definition
on selected cells
(sfGFP channel)ratiometric image
of segmented cells*lyz:Cxcr1-FT|lyz:mCFP*
wounded larva 1

METHOD 2:
Contour-based
membrane
segmentation
followed by
computation of
CFP/GFP ratio

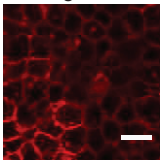
lyz:Cxcr1-FT|lyz:mCFP
wounded larva 2**D**

A**B****C****D**

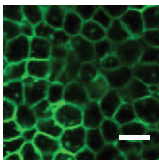
Receptor
+mCFP



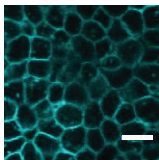
tagRFP



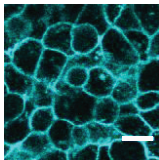
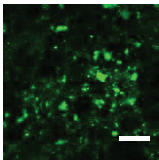
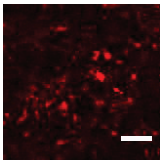
sfGFP



mCFP



Receptor
+ mCFP
+ Cxcl8a



Cxcr1-FT